

Dissipative Particle Dynamics Simulation on the Formation Process of CeO₂ Nanoparticles in Alcohol Aqueous Solutions

Qi Zhang, Jing Zhong*, Bao-Zhu Yang, Wei-Qiu Huang, Ruo-Yu Chen, Jun-Min Liao†, Chi-Ruei Gu†, and Cheng-Lung Chen†,*

School of Petrochemical Engineering, Jiangsu Province Key Lab of Fine Petrochemical Engineering, Changzhou University, Changzhou, 213164, Jiangsu, P.R. China. *E-mail: zjwyz@cczu.edu.cn

†Department of Chemistry, National Sun Yat-sen University, Kaohsiung, 80424, Taiwan, R.O.C.

*E-mail: chen1@mail.nsysu.edu.tw

(Received June 4, 2012; Accepted July 12, 2012)

ABSTRACT. Dissipative particle dynamics (DPD) was carried out to study the nucleation and crystal growth process of CeO₂ nanoparticles in different alcohol aqueous solutions. The results showed that the nucleation and crystal growth process of CeO₂ can be classified into three stages: nuclei growth, crystal stabilization and crystal aggregation except the initial induction stage, which could be reproduced by collecting simulation results after different simulation time. Properly selecting the sizes of CeO₂ and water bead was crucial in the simulation system. The influence of alcohol type and content in solutions, and precipitation temperature on the particle dimension were investigated in detail and compared with the experimental results. The consistency between simulation results and experimental data verify that the simulation can reproduce the macroscopic particle aggregation process. The effect of solvent on the nucleation and crystal growth of CeO₂ nanoparticles are different at three stages and can not be simply described by Derjaguin-Landau-Verwey-Overbeek (DLVO) theory or nucleation thermodynamics theory. Our work demonstrated that DPD methods can be applied to study nanoparticle forming process.

Key words: Dissipative particle dynamics, CeO₂ Particle dimension, Alcohol content, Precipitation temperature

INTRODUCTION

In recent years, nanometer-sized particle of cerium dioxide (CeO₂) has been widely used in many fields, such as gas sensor,¹ electrode materials for solid oxide fuel cells,² catalytic supports for automobile exhaust system,³ UV absorbent and filters⁴ and abrasives of the chemical mechanical polishing slurry,⁵ since CeO₂ particle has high stability at high temperature, high hardness and reactivity.⁶

Over the past decade, several techniques have been developed to produce the CeO₂ particles, such as: sol-gel process,⁷ hydrothermal synthesis,⁸ forced hydrolysis,⁹ microemulsion,¹⁰ electrochemical synthesis¹¹ and precipitation.¹²⁻²⁰ The liquid-phase precipitation method is more attractive among these techniques because the low cost salt precursors, simple operation and ease of mass production.¹⁷

In general, the liquid-phase precipitation process includes three stages: chemical reaction, nucleation, and crystal growth.¹³ These stages are fast in most cases, but difficult to control and observe in experiments. The dimension of CeO₂ particles formed in water by liquid-phase precipitation is in the range of 10-15 nm from XRD measurement.¹⁷

Some researchers reported that adding low dielectric medium, such as alcohols, to the aqueous solution could alter the thermodynamics of reaction system and nucleation kinetics in nanoparticle forming process, which lead the formation of particle with smaller size.^{16,18,19,21} Chen¹⁶ and Li et al.^{18,19} have reported that the particle size of CeO₂ decreased to 8-10 nm by introducing the monohydric alcohols - methanol (MeOH), ethanol (EtOH), iso-propanol (*i*-PrOH), *tert*-butanol (*t*-BuOH), into the aqueous solutions. The decrease of particle size varied with the type and quantity of alcohols adding into the aqueous solutions, and can be explained by the Derjaguin-Landau-Verwey-Overbeek (DLVO) theory and nucleation thermodynamics theory for crystal.

Chen et al.¹⁶ found that the particle size of CeO₂ decreases with the increasing of alcohol content in solutions, and the size of particle formed in 67 vol.% alcohol aqueous solutions at 50 °C decrease as MeOH aq > EtOH aq > *i*-PrOH aq ≈ *t*-BuOH aq. The order is directly proportional to the dielectric constant, ϵ , of solvent. In Li's work,^{18,19} they found the particle size of samples obtained in 75 vol.% alcohol aqueous solutions at 75 °C decreases in the order: *i*-PrOH aq > EtOH aq > MeOH aq > *t*-BuOH aq.

The order, however, is not proportional to the ε value of solvent. They also found there has a minimum particle size with the increasing of alcohol content in solutions. Their experimental results can not be explained simply by DLVO theory or nucleation thermodynamics theory for crystal. In addition to this, these two experiments are not consistent, which perhaps due to the different initial concentration of reactants and reaction time. It is difficult to measure the forming kinetics for CeO₂ nanoparticle because the formation process is too fast.

In addition to the experimental efforts, computer simulation is a possible way to study the phase separation and particle aggregation. Conesa investigated the structures and relative stabilities of several CeO₂ surfaces and of anion vacancy centers using theoretical molecular mechanics (MM) method. The simulations reproduce the experimental bulk modulus of CeO₂ within ~10% error.²² Gotte et al. simulated the bulk and (011) surfaces of reduced and unreduced CeO₂ by MD method, and concluded that the main structural change occurring on ceria reduction are the new equilibrium positions for the oxygen ions.²³ Baudin et al. studied the dynamics, structure and energetics of the (111), (011) and (001) surface of CeO₂ by molecular dynamics (MD) simulation method within *NPT* ensemble.²⁴ They reported the structure and defects of ceria without considering the forming process of CeO₂ nanoparticle.

For the nanoparticle forming process with solvents and metal-oxide molecules, the DPD method is especially appropriate because it is capable of studying systems containing millions of atoms in the nano-second time domain, and can describe adequately the phase separation process.²⁵⁻²⁸ The method was introduced by Hoogerbrugge and Koelman in 1992.²⁹ In our previous work, DPD have been used to simulate phase behaviors of EO₂₀PO₇₀EO₂₀ (P123) in water, ethanol/water solutions and silica sol.³⁰ The results indicated that DPD simulation method can be used to study the influence of template on the structure of mesoporous material and guide the preparation of mesoporous material. We also applied DPD to investigate the self-assembled aggregation problems of surfactants and a gold nanoparticle system,^{30,31} and found that the major difficulty to reproduce macroscopic experimental phase behavior by the simulation lies on the choosing of bead size and interaction parameters. Although Groot and Warren discussed the DPD method in detail and gave suggestions on the selection of DPD parameters,³² some fundamental problems still remained unclear. No consistent protocol has been reported to determine these two important parameters.

In this work, the growth of CeO₂ nanoparticle based on the precipitation process was simulated. The nucleation and crystal growth of the particles were investigated by using DPD simulation. The way to define DPD beads were discussed in the simulation section. To be consistent with the experimental works, various alcohol aqueous solutions: MeOH aq, EtOH aq, *i*-PrOH aq, *t*-BuOH aq, were used in the simulation. The effects of alcohol type, concentration, and precipitation temperature on the particle dimension were investigated. Our simulation provides a possible tool for the investigation of the nucleation and crystal growth of nanoparticles.

SIMULATION METHOD

Crystal Growth Theory

The growth of crystal is always analyzed by DLVO theory and nucleation thermodynamics theory. Based on the DLVO theory, the interaction potential between particles can be described as,¹⁹

$$V = \frac{A\kappa d}{6} + \pi\varepsilon\kappa d\psi^2 \quad (1)$$

where, A is Hamker constant; κ is Debye-Hückel parameter; d is the diameter of the particle; ψ is surface potential; ε is dielectric constant of solvents; and V is interactive potential between particles respectively. The first and second term in the equation represent electro-attractive and repulsive interactions respectively. According to this equation, the electrostatic repulsion force between particles would decrease with the decreasing of the ε values of solvents, which leads the particles easy to aggregate and growth. Therefore, within certain concentration range and at certain precipitation temperature, the particle dimension is inversely proportional to the ε values of solvents if the electrostatic repulsion force between particles dominated in the nanoparticle forming process.

On the other hand, the forming of particles strongly depends on the supersaturation of solute according to the nucleation thermodynamic theory, which can be expressed by Kelvin equation,³³

$$\ln S = \frac{4m\gamma}{dkT\rho} \quad (2)$$

where S is supersaturation of solute; m is the weight of solute molecule; γ is the interfacial energy between solute and solution phase; ρ is the density of solute; k is the Boltzmann's constant; and T is the Kelvin temperature respectively. Conventionally, S is defined as the ratio of solute

concentration (C) to the equilibrium concentration of solute (C_l) in the saturated solution.

$$S = \frac{C}{C_l} \quad (3)$$

According to Debye-Hückle theory, C_l can be expressed as:¹⁶

$$C_l \approx \exp\left[\frac{z_+z_-e^2}{4\pi\epsilon_0\epsilon kT(r_+r_-)}\right] \quad (4)$$

where ϵ_0 is the permittivity in vacuum and ϵ is the dielectric constant in a given solution; r_+ and r_- represent the radius of ions charged z_+ and z_- respectively; and e represents the elementary charge ($e = 1.602 \times 10^{-19}$ C).

In combination of equations (2), (3) and (4) yields,

$$\frac{4m\gamma}{dkT\rho} = \ln C + \frac{z_+z_-e^2}{4\pi\epsilon_0\epsilon kT(r_+r_-)} \quad (5)$$

From this equation, the particle size was directly proportional to the ϵ value of solvents if the supersaturation of solute controlled the nanoparticle forming process.

Based on the above analysis, a change in ϵ value of solvent can alter the electrostatic repulsion forces between particles and the supersaturation of solute in the opposite direction.

DPD Theory

The outline of the DPD model here is based on the work by Groot and Warren.³² Molecules are divided into beads, and the motions of beads are governed by Newton's equations:

$$\frac{d\vec{r}_i}{dt} = \vec{v}_i \quad (6)$$

$$\frac{d\vec{v}_i}{dt} = \vec{f}_i \quad (7)$$

where \vec{r}_i , \vec{v}_i , \vec{f}_i are the position vector, velocity and total force on the i th bead respectively. The total force exerted on bead i contains three parts.

$$F_i = \sum_{i \neq j} (F_{ij}^C + F_{ij}^D + F_{ij}^R) \quad (8)$$

where F_{ij}^C is the conservative force which describe soft repulsive central force between bead i and j ; F_{ij}^D and F_{ij}^R are the dissipative and random forces respectively. The significance of these terms is investigated in detail elsewhere.^{29,32}

To simulate a system, a set of interacting parameters

α_{ij} 's between different types of beads must be determined. The DPD simulation should reproduce correct phase behaviors as observed experimentally with these pre-determined parameters. There are several methods suggested in the literature to evaluate interaction parameters.³⁴ We adopted Monte Carlo method to evaluate the interaction parameters by compromising the accuracy and computation time. The derivation of α_{AB} is based on Flory-Huggins mixing parameter χ_{AB} where the subscript AB denotes type A and B beads,³⁵ which is related to the mixing energy by

$$\chi_{AB}(T) = E_{AB}^{mix}(T)/RT \quad (9)$$

The maximum repulsion α_{AB} deduced from this χ_{AB} parameter at a given particle density $\rho = N/V$, as suggested by Groot and Warren.³²

$$\alpha_{AB}(T) = \alpha_{AA} + 1.451\chi_{AB}(T) \quad \text{for } \rho = 5 \quad (10)$$

$$\alpha_{AB} = \alpha_{AA} + 3.497\chi_{AB}(T) \quad \text{for } \rho = 3 \quad (11)$$

The α_{AA} term is derived from the compressibility of pure component A ($\alpha_{AA} = 75k_B T/\rho$).³² All simulations were performed with Cerius2 and Material Studio software packages.³⁶

Determination of Simulation Parameters

To carry out DPD simulation, molecular fragments are usually treated as beads. There is no definitive way to divide the chain molecule into fragments. In the first attempt, the molecules of MeOH, EtOH, *i*-PrOH, *t*-BuOH, EG, water and CeO₂ are directly used as beads for DPD simulation. The structures of these molecules were optimized with UNIVERSAL force field (UFF).³⁷ All atomic partial charges of molecules were obtained from quantum mechanical ZINDO method based on the optimized structures except CeO₂ molecule. The atomic partial charges of CeO₂ molecule was calculated by the Density Functional Theory (DFT) with Gaussian 03 software.³⁸ The hybrid and correlation functionals B3LYP and SDD potential form was used. The interacting parameter χ_{AB} was calculated by UFF.³⁷ These DPD simulations failed to reproduce aggregation behavior as observed experimentally. This was because the sizes of CeO₂ and water are too much smaller than those of alcohols.

To generate CeO₂ bead with its size comparable to the alcohols, a small CeO₂ cluster with fluorite structure containing two CeO₂ molecules was adopted to represent CeO₂ bead. Similarly, a water cluster with cubic ice crystal

Table 1. (a) Interaction parameters of beads in the simulation systems at 50 °C

a_{ij}	CeO ₂ bead	MeOH	EtOH	<i>i</i> -PrOH	<i>t</i> -BuOH	EG	Water bead
CeO ₂ bead	15.000	76.866	79.929	80.366	80.813	64.136	64.324
MeOH	76.866	15.000	15.124	15.403	15.607	15.289	15.907
EtOH	79.929	15.124	15.000	15.029	15.135	15.327	16.587
<i>i</i> -PrOH	80.366	15.403	15.029	15.000	14.994	15.410	17.074
<i>t</i> -BuOH	80.813	15.607	15.135	14.994	15.000	15.458	17.429
EG	64.136	15.289	15.327	15.410	15.458	15.000	15.559
Water bead	64.324	15.907	16.587	17.074	17.429	15.559	15.000

(b) Interaction parameters of beads in the simulation systems at 75 °C

α_{ij}	CeO ₂ bead	MeOH	EtOH	<i>i</i> -PrOH	<i>t</i> -BuOH	EG	Water bead
CeO ₂ bead	15.000	72.087	74.732	75.259	75.917	60.878	60.870
MeOH	72.087	15.000	15.139	15.344	15.562	15.262	15.825
EtOH	74.732	15.139	15.000	15.062	15.149	15.294	16.452
<i>i</i> -PrOH	75.259	15.344	15.062	15.000	14.999	15.337	16.848
<i>t</i> -BuOH	75.917	15.562	15.149	14.999	15.000	15.425	17.222
EG	60.878	15.262	15.294	15.337	15.425	15.000	15.569
Water bead	60.870	15.825	16.452	16.848	17.222	15.569	15.000

structure containing two water molecules was choosing to represent water bead. Table 1(a) and 1(b) shows the calculated interaction parameters α_{AB} 's of CeO₂, water bead and various alcohols at 50 and 75 °C.

All systems were simulated at the particle density $\rho = 5$. A 3D box of size 30×30×30 DPD units with periodic boundary conditions was adopted in the simulation. The dissipative parameter γ_{ij} was set to a value of $4.5k_B T$, and the time step Δt was set as 0.05 according to Ref. 35. 100,000 time steps were carried out for each system, and the molar ratio of [CeO₂]:[solvent] was kept at 0.20. The initial conformations and velocities were random. After comparing many times of simulations, we found the repeatability was good. Therefore, the parameters adopted in our simulation are reasonable and the conclusions are reliable. In addition, this parameterization method has been also used in wide-range systems on DPD simulation, such as: self-assembled aggregation problems of surfactants,^{39,40} gold nanoparticle system,³¹ etc., and gives good results.

RESULTS AND DISCUSSION

The particle sizes of CeO₂ formed in different alcohol aqueous solutions and at different simulation time were evaluated and compared with experimental results. The effects of volume content of alcohol in solutions and precipitation temperature on the particle sizes were also investigated.

Growth Process of CeO₂ in Alcohol Aqueous Solutions

Giving in Fig. 1 are snapshots of the CeO₂ particles formed in MeOH aq solutions at different simulation time. The red bead represents the CeO₂, and the solvent was neglected in all Figures for clarity. The simulation temperature was set at 50 °C, and 50 vol.% MeOH aq solution was used. The results show that CeO₂ molecules can form spherical aggregated particles at different simulation time. The number of aggregated particles decreased with the increasing of simulation time, but the dimension of particles increased, which reproduced the aggregation process in the precipitation experiments in alcohol aqueous solutions. The relationships of particle dimension and aggregation number are similar in other alcohol aqueous solutions.

Fig. 2 shows the dimensions of particles formed in different 50 vol.% alcohol aqueous solutions at 50 °C. The particle size was calculated by averaging the radial length of particle in *x*, *y* and *z* directions. According to the dimension of molecules defined for DPD beads and the particle density $\rho = 5$ used in the simulation, a DPD unit is about 0.74 nm. Then the particle size can be transferred from DPD unit into "nm" unit.

The process of CeO₂ particles formed in monohydric alcohols (MeOH, EtOH, *i*-PrOH, *t*-BuOH) has been simulated with the increasing simulation time. In the first 10,000 time steps, nuclei had been already formed. Between 10,000 time steps and 30,000 time steps, the dimensions of CeO₂ particles grow rapidly. This is because the particles were near to each other. After the fast growth stage, the

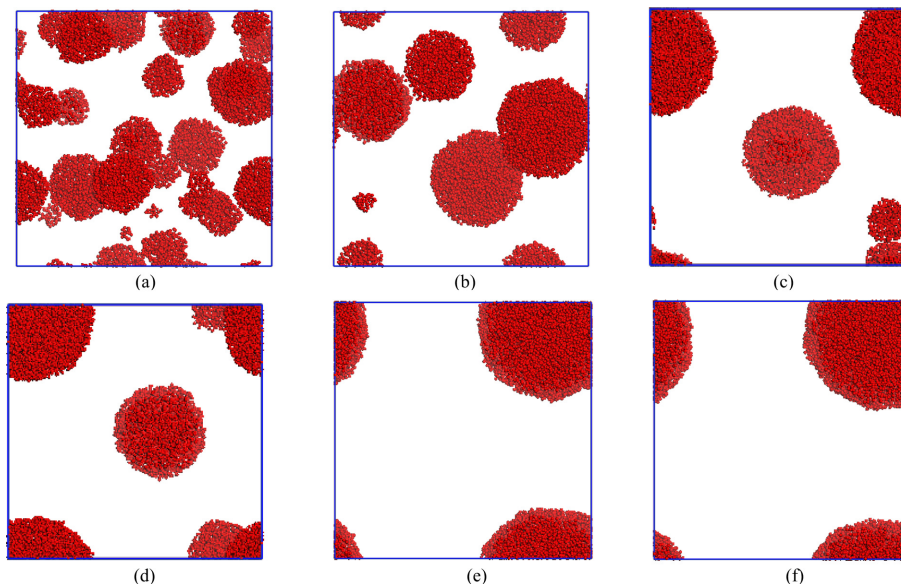


Fig. 1. Simulation results of CeO₂ particles at different simulation time (50 °C, MeOH/water = 50 vol.%, molar ratio of [CeO₂]: [solvent] = 0.20) (a)10,000; (b) 30,000; (c) 50,000; (d) 70,000; (e) 90,000; (f) 100,000.

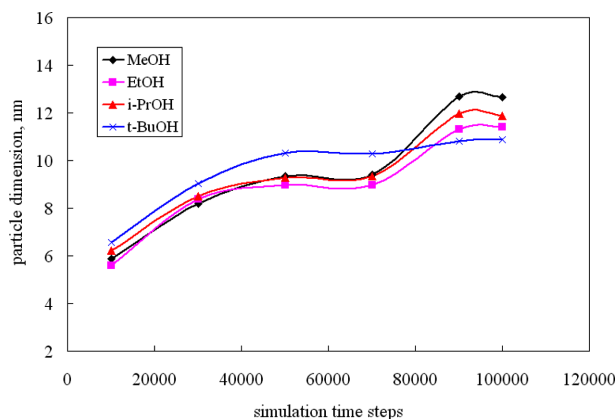


Fig. 2. Dimension of CeO₂ particles formed at different simulation time (50, alcohol/water = 50 vol.%, molar ratio of [CeO₂]:[solvent] = 0.20).

particles grow gently until 70,000 time steps; since grown particles were already separated in distance from each other. After 70,000 time steps, the dimensions of the particles increased rapidly. This result indicates that the aggregation happened between those large particles.

Comparing the simulated dimension of the CeO₂ particles with the experimental measured size from XRD measurement,¹⁶⁻¹⁹ we found that the sizes of CeO₂ particles formed within 30,000 time steps are very close to the measured sizes of CeO₂ single crystal.^{16,18,19} Therefore the particles formed within 30,000 time steps have not finished the nuclei growth. After this point, further nucleation occurred between particles, and this stage can be classified as nuclei

growth stage. The size of particle increased gently when the simulation time extend from within 30,000 to 70,000 time steps, which indicated that the CeO₂ crystals formed in alcohol aqueous solutions were stable in a certain period. This stage can be classified as stabilization stage. The size of particles after 70,000 steps is much larger than that of single crystal from XRD results. This stage can be classified as aggregation stage. Our simulation shows that the growth of CeO₂ particle in the alcohol aqueous solutions undergoes different stages.

Effect of Alcohol Type in Alcohol Aqueous Solutions

The dimension of particles formed at different simulation time also depends on the type of alcohol as shown in Fig. 2. The size of CeO₂ particle are in the order *t*-BuOH(aq) > *i*-PrOH(aq) > EtOH(aq) > or ≈ MeOH(aq) when the simulation time less than 30,000 time steps (in nuclei growth stage), which is almost inversely proportional to the ϵ values of alcohol solutions. The trend is quite consistent with the results reported by both Hu et al.²¹ and Chen et al.¹⁶ They studied the relationship between incubation time and average hydrodynamic diameter of zirconia particles in different alcohol(aq) solutions at equal concentrations of alcohol and water (50 vol.%), and found that the nucleation rate of zirconia particles in different alcohol solutions were in the order *i*-PrOH(aq) > EtOH(aq) > MeOH(aq) after the initial induction stage. Therefore, we can deduce that the particle growth was controlled by electrostatic repulsion between particles in this stage because the particle dimension

was inversely proportional to the ε values of alcohol solutions.

In the range of 30,000 to 70,000 time steps (crystal stabilization stage), we found that the dimension of CeO₂ particles grows gently independent of type of alcohol. This indicated that electrostatic repulsion between particles still dominant the forming of particles in the crystal stabilization stage.

When simulation time is more than 70,000 time steps (crystal aggregation stage), the order of particle size changed abruptly, which decreases as following sequence: MeOH(aq) > *i*-PrOH(aq) > EtOH(aq) > *t*-BuOH(aq). This indicates that the mechanism of particle formation changed in this stage. Within this range the order of particle size is almost directly proportional to the ε values of alcohol(aq) solutions except the EtOH(aq), which indicated that the crystal growth of CeO₂ was controlled by the supersaturation of CeO₂ in the solutions according to the nucleation thermodynamic theory. The order of particle size obtained in our simulation is quite consist with the experimental results reported by Chen et al. at the same experimental conditions,¹⁶ but the simulated particle sizes are slightly larger than the reported values, which perhaps due to the vigorous stirring in the experiments inhibiting the aggregation of CeO₂ particles.

The consistency of simulation results with the experimental results in monohydric alcohol(aq) solutions indicates that DPD simulation can describe the sequential forming process of CeO₂ nanoparticle, including nuclei growth, crystal stabilization and crystal aggregation stages. We can also infer that the growth of particle at the nuclei growth and crystal stabilization stages was controlled by electronic repulsion between particles, which can be described by DLVO theory; and the growth of particle at the crystal aggregation stage was controlled by the supersaturation of CeO₂ in the solutions, which can be described by nucleation thermodynamics theory. In other words, the nuclei growth and crystal repairing is faster for molecules in solvents with lower ε values, and the crystal aggregation is slower for particle in solvents with lower ε value. The two mechanisms are effective in the whole particle growth process and compete with each other.

Effect of Alcohol Content in Alcohol Solutions

The ε value of solvents can be adjusted by changing the content of alcohol in the alcohol(aq) solutions. The addition of alcohol into water would decrease the ε value and the dissolvent ability of solvents. The solution is therefore supersaturated and capable of producing finer particle.²¹ On the other hand the electrostatic repulsion between

particles would decreases with the decreasing of the ε value, which leads to form larger CeO₂ particles. Chen et al.¹⁶ and Li et al.¹⁸ reported the effect of alcohol/water ratio on the dimension of CeO₂ particle in separated works. Chen et al. found that the dimension of particle decreases with the increasing of alcohol/water ratio.¹⁶ While Li et al. found a minimum value in particle dimension during the increasing of EtOH(aq) ratio.¹⁸

The effect of alcohol/water ratio on the dimension of CeO₂ nanoparticle by DPD at 50 °C was studied, and the results are shown in Figs. 3-5. Fig. 3 gives the size of particles formed after 30 000 simulation steps. We found that the effect of alcohol/water ratio on the dimension of CeO₂ particle was varied with the alcohol type used in solutions. The general trend, except EtOH(aq), is the size of CeO₂ particle decreases with the increasing of alcohol/water ratio, but the change details are different for different solvents.

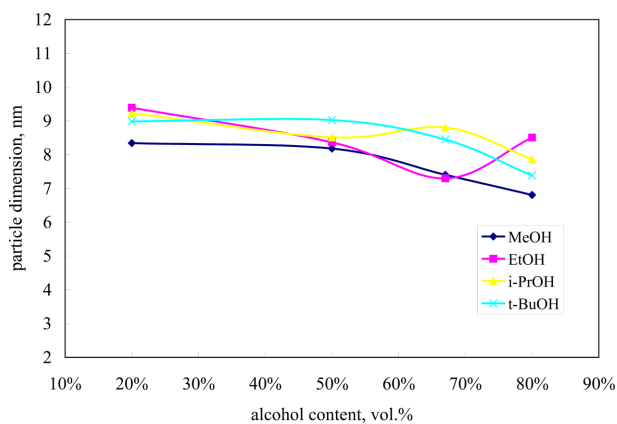


Fig. 3. Dimension of CeO₂ particles formed in different alcohol/water mixed solvents (50 °C, molar ratio of CeO₂/solvent = 0.20, 30,000 time steps).

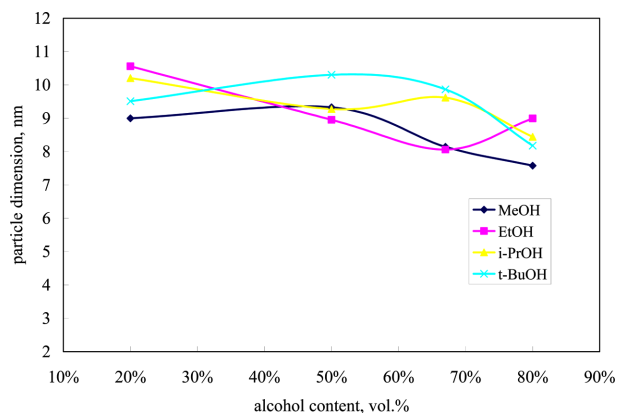


Fig. 4. Dimension of CeO₂ particles formed in different alcohol/water mixed solvents (50 °C, molar ratio of CeO₂/solvent = 0.20, 50,000 time steps).

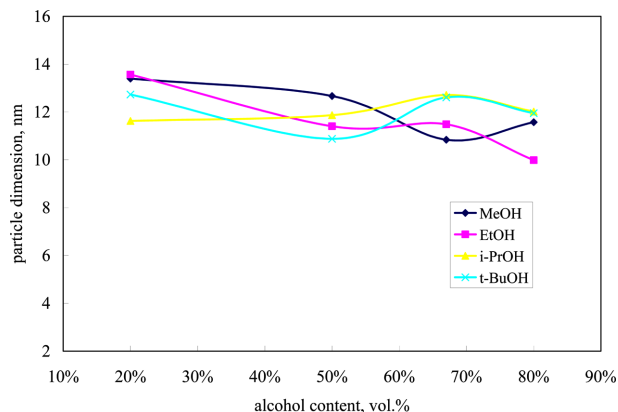


Fig. 5. Dimension of CeO₂ particles formed in different alcohol/water mixed solvents (50 °C, molar ratio of CeO₂/solvent = 0.20, 100,000 time steps).

For the particles formed in MeOH(aq) and *t*-BuOH(aq), the change trends of particle sizes are almost consistent when the alcohol content in solutions raised from 20 vol.% to 50 vol.%, then decreased when the alcohol content larger than 50 vol.% after 30,000 time steps simulation. This indicates that the effect of electrostatic repulsion and that of supersaturation of CeO₂ reach equilibrium when the alcohol content was in the range of 20 vol.% to 50 vol.%, but the effect of supersaturation of CeO₂ become dominant when the alcohol content in solutions larger than 50 vol.%. In *i*-PrOH(aq), the particle dimension decreases with the increasing of alcohol content in the range of 20% to 50%, and slightly increases in the range of 50 vol.% - 67 vol.%, then drop obviously in the range of 67-80 vol.% after 30,000 time steps simulation. This indicates that the supersaturation of CeO₂ almost dominate the whole process. The effect of electrostatic repulsion was only significant within the range of 50 vol.% to 67 vol.% alcohol content. In the EtOH(aq), there existed a minimum point in the curve of particle dimension vs. the alcohol content. Therefore, the supersaturation of CeO₂ control the forming of particles in the initial particle forming stage, then the electrostatic repulsion become dominant when the alcohol content was larger than 67 vol.%. This trend is as same as reported by Li et al.¹⁹ and confirmed that our simulation can reproduce the effect of alcohol content in alcohol(aq) solutions on the particle dimension.

When the simulation time extend to 50,000 time steps, the sizes of particles formed in MeOH(aq) and *t*-BuOH(aq) become larger when the alcohol content in alcohol(aq) solutions raised from 20 vol.% to 50 vol.% as shown in Fig. 4. This indicates that the equilibrium between electrostatic repulsion and supersaturation of CeO₂ at 30,000 time

steps was shifted and the electrostatic repulsion became dominant. For other alcohols and alcohol content, the relationship between particle size and alcohol content in alcohol(aq) solutions is almost unchanged though the particle size increase when the simulation steps prolonged to 50,000 steps, This indicates that the influence of alcohol content on the particle size is similar for nuclei growth stage and crystal stabilization stage.

The change of particle dimension with alcohol content in alcohol(aq) solutions after 100,000 time steps is different with those after 30,000 time steps and 50,000 time steps as shown in Fig. 5. There exists the minimum or maximum point for almost all the alcohol(aq) solutions studied in our simulation, which indicates that electrostatic repulsion force and supersaturation of CeO₂ still compete with each other and one of these two factors controls the aggregation.

The effect of alcohol content in alcohol(aq) solutions on the particle dimension shows some irregular phenomena because electrostatic repulsion forces and supersaturation of CeO₂ in solution competed with each other in different alcohol solutions. The trend of nanoparticle in the crystal forming stage can not be predicted by any simple theory. Our DPD simulation, however, can reproduce the experimental results on the dimension of CeO₂ nanoparticle. The method is adequate to investigate such problems.

Effect of Precipitation Temperature

The increase of temperature would decrease the ε value of alcohol,²¹ and increase the supersaturation of CeO₂. Therefore temperature increasing would decrease the size of the nanoparticle. So the simulation in nuclei growth stage (less than 30,000 time steps) was investigated in this part.

The dimension of CeO₂ particle decreases when the simulation temperature increased from 50 °C to 75 °C in alcohol(aq) solutions with 50 vol.% alcohol as shown in Fig. 6, which consisted with the rule deduced from the relationship between supersaturation and temperature. The other interesting phenomenon occurred with the increasing of temperature is that the relationship between particle size and different alcohol solutions. The order of particle size changed from *t*-BuOH(aq) > *i*-PrOH(aq) > EtOH(aq) > MeOH(aq) to *i*-PrOH(aq) > MeOH(aq) > EtOH(aq) \approx *t*-BuOH(aq) with the increasing of temperature. This indicated that supersaturation of CeO₂ also became important for particle growth. This phenomenon become obviously at 75 °C and alcohol/water = 75 vol%. The dimension of particle shows a maximum value in *i*-PrOH(aq) at 75 °C and *i*-PrOH(aq) = 75 vol%, which consisted with the

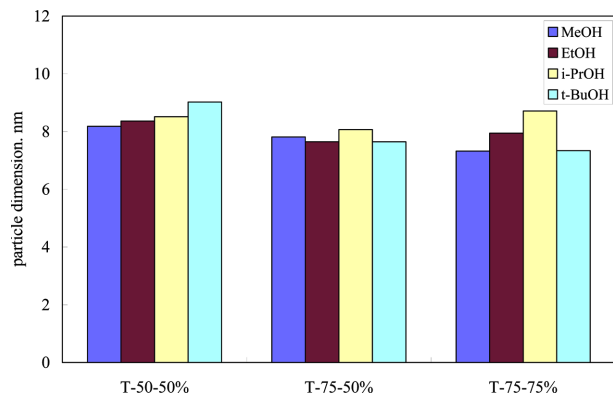


Fig. 6. Dimension of CeO₂ particles formed at different temperature (molar ratio of CeO₂/solvent = 0.20, 30,000 time steps).

experimental results reported by Li et al.¹⁹ at the same experimental conditions. This consistency confirmed that our DPD simulation can correctly reproduced experimental results at different temperature.

The effect of alcohol content in the alcohol(aq) solutions on the particle size is also investigated at 75 °C. After 30,000 time step, the dimension of particles formed in MeOH(aq) decreases when the alcohol content increased from 50 vol.% to 75 vol%; increases slightly in EtOH(aq), and increases markedly in *i*-PrOH(aq); but decreases in *t*-BuOH(aq). The irregular trends is similar with the phenomena observed at 50 °C, and can be explained by the competition between electrostatic repulsion force and the supersaturation of CeO₂ in solutions which influence the particle dimension contrarily. The detail in mechanism need further study.

CONCLUSION

DPD simulation was carried out to investigate the forming process of CeO₂ nanoparticle in alcohol(aq) solutions. The formation can be divided into nuclei growth, crystal stabilization and crystal aggregation, which can be observed by collecting the simulation results at different simulation time. The nuclei growth stage within the range of less than 30,000 time simulation steps, and the particles grew rapidly in this stage; crystal stabilization stage is within the range of 30,000 and 50,000 simulation time steps, and the size of particle remains unchange in this stage; particle aggregation is within the range after 50,000 simulation time steps, the particles further aggregate and the dimension of particles was larger than that of single crystal.

The dimension of CeO₂ nanoparticle is inversely pro-

portional to the ϵ value of alcohol(aq) solutions, and electrostatic repulsion force between particles controls the forming process when the CeO₂ nanoparticle is in the nuclei growth stage; and that would change to be directly proportional to the ϵ value of alcohol(aq) solutions and the supersaturation of CeO₂ in solutions controls the forming process when the CeO₂ nanoparticle has entered into the crystal aggregation stage. The precipitation kinetics is faster for molecules in solvents with lower ϵ values, and the crystal aggregation kinetics is slower for particle in solvents with lower ϵ value.

The particle dimension decreases with the increasing of alcohol content in alcohol(aq) solutions and temperature when the particles were in the nuclei growth stage. The effect of alcohol content in alcohol(aq) solutions on the CeO₂ particle dimension is irregular because the two actions – electrostatic repulsion force between particles and the supersaturation of CeO₂ in solutions would compete with each other during the change of alcohol content and influence the particle dimension contrarily.

The simulation results produce from different type and content of alcohol in alcohol(aq) solutions, and different temperatures consist with the experimental data obtained at same conditions. Our work has demonstrated that DPD methods can be applied to the study of nanoparticle forming process.

Acknowledgments. This work is supported by the Project Funded by the Priority Academic Program Development of Jiangsu Higher Education Institutions, the Natural Science Foundation of Jiangsu Province (BK2011240), Major Projects of Natural Science Research of Colleges and Universities in Jiangsu Province (11KJA610002), the Transformation of Scientific and Technological Achievements and Industrialization plan (Innovation Funds) of Changzhou (CC20110003), the Jiangsu College Graduate Research and Innovation Projects (CXZZ11_0374).

REFERENCES

- Izu, N.; Shin, W.; Murayama, N.; Kanzaki, S.; *Sensors and Actuator B: Chemical* **2002**, *87*, 95.
- Yahiro, H.; Baba, Y.; Eguchi, K.; Arai, H. *J. Electrochem. Soc.* **1988**, *135*, 2077.
- Kašpar, J.; Fornasiero, P.; Hickey, N. *Catal. Today* **2003**, *77*, 419.
- Yamashita, M.; Kameyama, K.; Yoshida, S.; Fujishiro, Y.; Kawai, T.; Sato, T. *J. Mater. Sci.* **2002**, *37*, 683.
- Jiang, M.; Wood, N. D.; Komanduri, R. *J. Eng. Mater.*

- Technol. (Trans. ASME)* **1998**, *120*, 304.
6. Zhou, X. D.; Huebner, W.; Anderson, H. U. *Appl. Phys. Lett.* **2002**, *80*, 3814.
 7. Chu, X.; Chung, W.; Schmidt, L. D. *J. Am. Ceram. Soc.* **1993**, *76*, 2115.
 8. Hirano, M.; Kato, E. *J. Am. Ceram. Soc.* **1999**, *82*, 786.
 9. Hsu, W. P.; Ronnquist, L.; Matijevic, E. *Langmuir* **1988**, *4*, 31.
 10. Masui, T.; Fujiwara, K.; Machida, K. I.; Adachi, G. Y.; Sakata, T.; Mori, H. *Chem. Mater.* **1997**, *9*, 2197.
 11. Zhou, Y.; Phillips, R. J.; Switzer, J. A. *J. Am. Ceram. Soc.* **1995**, *78*, 981.
 12. Djuričić, B.; Pickering, S. J. *Eur. Ceram. Soc.* **1999**, *19*, 1925.
 13. Zhou, X. D.; Huebner, W.; Anderson, H. U. *Chem. Mater.* **2003**, *15*, 378.
 14. Li, Q.; Han, Z. H.; Shao, M. W.; Liu, X. M.; Qian, Y. T. *J. Phys. Chem. Solids* **2003**, *64*, 295.
 15. Chen, J. Q.; Chen, Z. G.; Li, J. C. *J. Mater. Sci. Technol.* **2004**, *20*, 438.
 16. Chen, H. I.; Chang, H. Y. *Colloids Surf., A* **2004**, *242*, 61.
 17. Chen, H. I.; Chang, H. Y. *Ceram. Int.* **2005**, *31*, 792.
 18. Li, X. Z.; Chen, Z. G.; Chen, J. Q.; Chen, Y.; Ni, C. Y. *J. Rare Earths* **2005**, *23*, 321.
 19. Li, X. Z.; Chen, Y.; Chen, Z. G.; Chen, J. Q. *Electronic Components & Materials* **2006**, *25*, 43.
 20. Chen, P. L.; Chen, I. W. *J. Am. Ceram. Soc.* **1993**, *76*, 1577.
 21. Hu, M. Z. C.; Payzant, E. A.; Byers, C. H. *J. Colloid Interface Sci.* **2002**, *222*, 20.
 22. Conesa, J. C. *Surf. Sci.* **1995**, *339*, 337.
 23. Gotte, A.; Hermansson, K.; Baudin, M. *Surf. Sci.* **2004**, *552*, 273.
 24. Baudin, M.; Wójcik, M.; Hermansson, K. *Surf. Sci.* **2000**, *468*, 51.
 25. Cao, X. R.; Xu, G. Y.; Li, Y. M.; Zhang, Z. *J. Phys. Chem. A* **2005**, *109*, 10418.
 26. Liu, H.; Qian, H. J.; Zhao, Y.; Lu, Z. Y. *J. Chem. Phys.* **2007**, *127*, 144903.
 27. Soto-Figueroa, C.; Vicente, L.; Martinez-Magadán, J.; Rodriguex-Hidalgo, M. *J. Phys. Chem. B* **2007**, *111*, 11756.
 28. Lisal, M.; Brennan, J. K.; Smith, W. R. *J. Chem. Phys.* **2006**, *125*, 164905.
 29. Hoogerbrugge, P.; Koolman, J. *Europhys. Lett.* **1992**, *19*, 155.
 30. Chen, Y.; Zhong, J.; Huang, W. Q.; Chen, R. Y.; Hu, W. H.; Chen, C.-L. *Chem. J. Chinese Universities* **2010**, *31*, 1827.
 31. Juan, S. C. C.; Hua, C. Y.; Chen, C. L.; Sun, X. Q.; Xi, H. T. *Mol. Simul.* **2005**, *31*, 277.
 32. Groot, R. D.; Warren, P. B. *J. Chem. Phys.* **1997**, *107*, 4423.
 33. Mullin, J. W. *Crystallization*; Butterworth-Heinemann: Boston, U.S.A., 1993.
 34. Bicerano, J. *Prediction of Polymer Properties*, 2nd ed.; Marcel Dekker: New York, 1996.
 35. Flory, P. *Principles of Polymer Chemistry*; Cornell University Press: Ithaca, 1953.
 36. *Materials Studio 4.2*; Discover/Accelrys: San Diego, CA, 2007.
 37. Rappé, A. K.; Casewit, C. J.; Colwell, K. S.; Goddard III, W. A.; Skiff, W. M. *J. Am. Chem. Soc.* **1992**, *114*, 10024.
 38. Frisch, M. J.; Trucks, G. W.; et al. *GAUSSIAN 03 revision D.02*; Gaussian, Inc.: Wallingford, CT, 2004.
 39. Ryjkitia, E.; Kuhn, H.; Rehage, H.; Muller, F.; Peggau, J. *Angew. Chem. Int. Ed.* **2002**, *41*, 983.
 40. Kuo, M. Y.; Yang, H. C.; Hua, C. Y.; Mao, S. Z.; Deng, F.; Wang, W. W.; Du, Y. R. *Chem. Phys. Chem.* **2004**, *5*, 575.
-